Ancient TL, Volume 7 No.1 1989

Alpha dose rate calculations in speleothem calcite: values of η and k_{eff}/k_{ref}

R. G. Lyons* and B. J. Brennan‡
Departments of Geography* and Physics‡, University of Auckland,
New Zealand.

The dose rate calculations for the age equation in ESR and TL dating must allow for the dependence of signal intensity produced by alpha radiation on alpha track length rather than on total energy deposited (Zimmerman, 1971; Aitken and Bowman, 1975; Lyons, 1988). Correction must also be made for any departure from linearity in the signal intensity *vs* track length response curve. In the *k* system of Zimmerman (1971) this is achieved by the use of k_{eff} instead of *k*, assuming the radionucleide chain is in equilibrium. In the *a* or *b* system (Aitken and Bowman, 1975; Bowman and Huntley, 1984) it is allowed for, firstly by using track length as the independent variable and, secondly, by applying the correction factor η.

At the 2nd International Symposium in ESR Dating and Dosimetry (held in Münich, October 1988), we presented the results of a study on alpha effectiveness including values for k_{eff}/k_{ref} and η in ESR dating for speleothem calcite which are up to 7% lower than the best estimates previously available (from the average of estimates for other materials). We believe these estimates to be the first direct calibrations for calcite. The magnitude of the difference that these correction factors will make to age estimates will depend, of course, on the relative contribution that the alpha dose makes to the total environmental dose-rate. Details of the methodology and details of calculation will be published in the Munich conference proceedings. However, because the error introduced by using the average estimate for other materials is systematic, we feel it is important that these figures be made available as soon as possible.

We used a small research nuclear accelerator as a source of alpha particles of various energies, as described in Lyons (1985, 1988), to determine the ESR response to alpha particles of different energies. Because of the nature of ESR measurement we were able to use alpha-thick instead of alpha-thin targets; the irradiating alpha particles were totally absorbed in the target, thus simulating the effect of internally produced alpha particles in a sample. This gave us the ESR response for alpha particles of the selected energies directly, without the need for further assumptions or calculations. In contrast, when thin targets are used, δ signal/ δ range is measured and integrated to obtain the signal/range curve, and therefore will incorporate any uncertainty in the signal response for low energies, the most difficult values to obtain experimentally (Bowman, 1976; Aitken and Bowman, 1975). A preliminary data set was presented in Lyons (1987, 1988). Here we present the full data set and summarize briefly the implications for alpha dose-rate calculations.

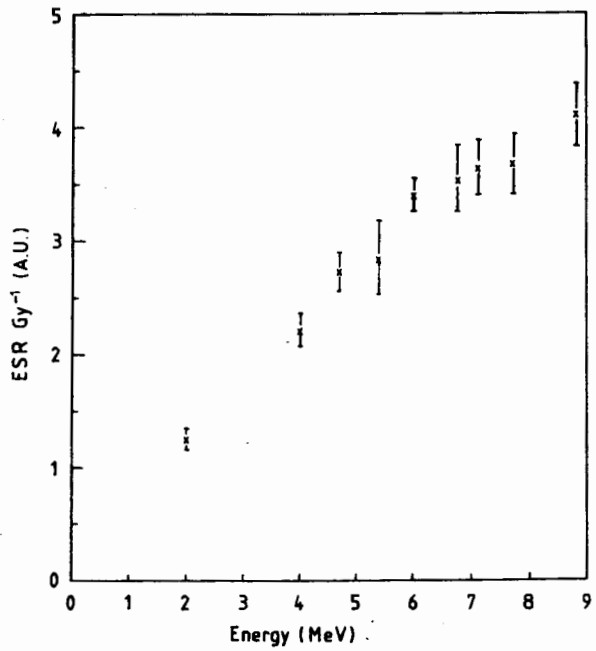

Figure 1. ESR per Gy versus energy of the incident alpha particles for a calcite speleothem sample.

Figure 1 shows that the ESR response per Gy of deposited energy depends on the energy of the irradiating alpha particle; Figure 2 shows that the total ESR response for an alpha particle which is completely absorbed in the sample, is an approximately linear function of the range of the alpha particle. Values for the range of alpha particles in calcium carbonate were calculated from data for stopping powers given in Zeigler (1977). Whereas the preliminary data set published in Lyons (1987) suggested that the response curve could be represented by a straight line passing through the origin, the full data set is best represented, for the range of energies occurring in the natural environment (i.e. for energies above 3 MeV), by a straight line with a non-zero intercept.

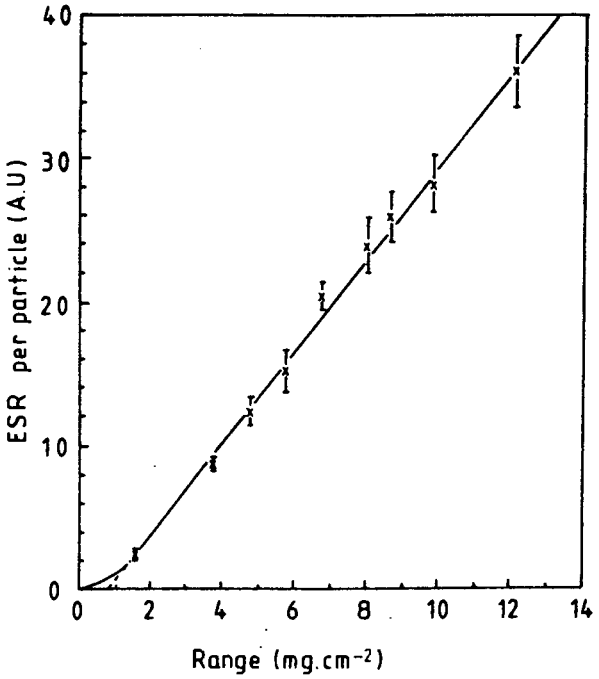

Figure 2:
ESR per particle versus range of the incident alpha particle for a calcite speleothem sample.

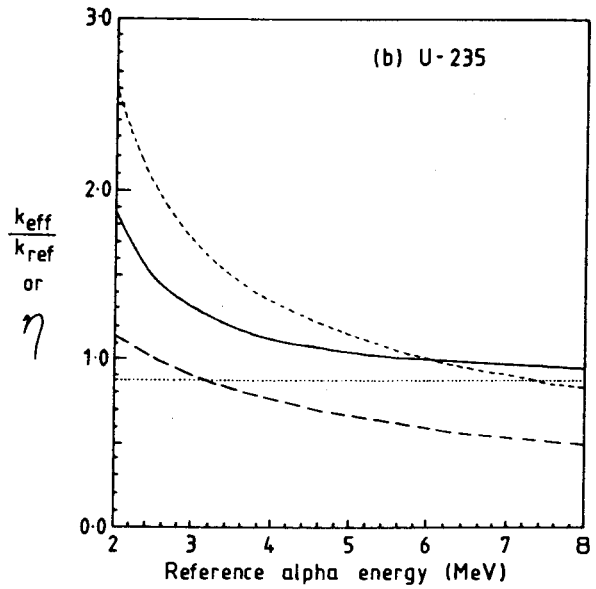

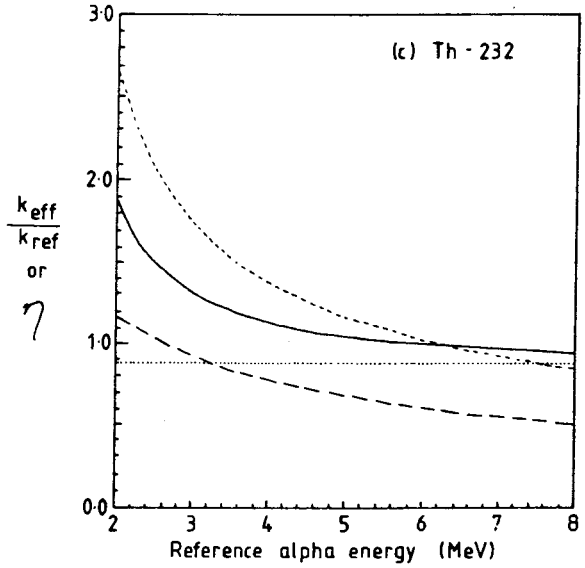

Figure 3:
Correction factors for calcite, for thick and thin calibration targets, a or b, and k systems as a function of reference energy: (a) U-238 chain in equilibrium; (b) U-235 chain in equilibrium, (c) Th-232 in equilibrium, and (d) U-238, assuming 100% radon escape.

- - - k_{eff}/k_{ref}, *thick target calibration*
_ _ _ k_{eff}/k_{ref}, *thin target calibration*
---- η, *thick target calibration*
..... η, *thin target calibration*

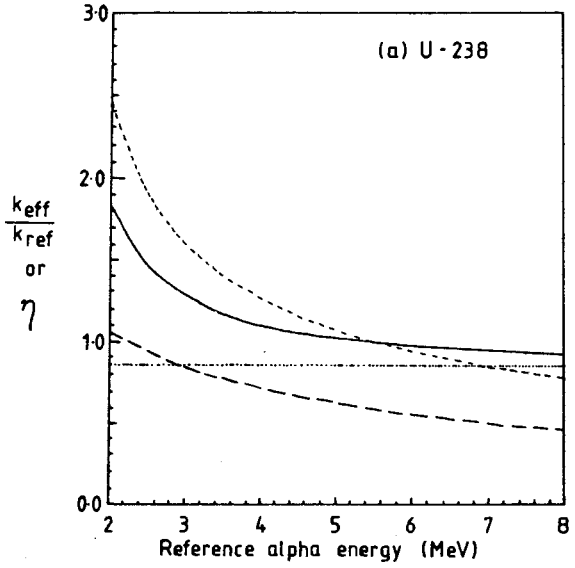

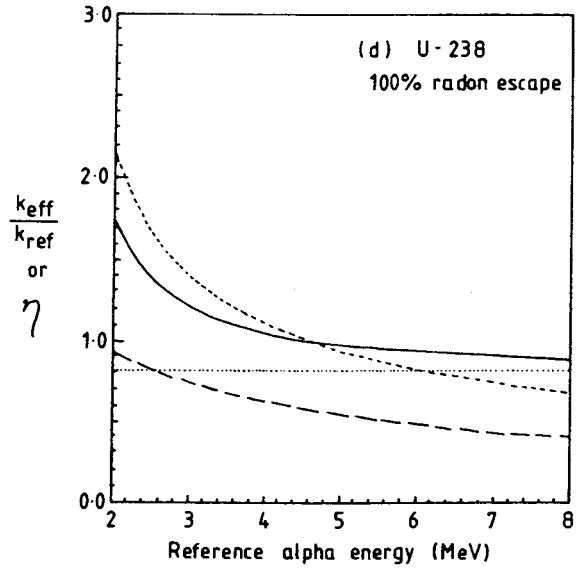

The implications for dose rate calculations are:

(i) confirmation that track length, not energy, should be the fundamental variable in dose rate calculations for ESR as well as TL. The direct application of dose rate tables expressed in terms of energy, such as given in Bell (1979) or Nambi and Aitken (1986) is incorrect.

(ii) a correction term should be subtracted from the track length for each alpha energy present, to allow for the non-zero intercept and thus give the 'effective track length' for use in the dose rate calculation. In the case of speleothem calcite, we estimate the subtraction term to be 0.875 $mg.cm^{-2}$. The uncertainty in this correc-tion term is no more than 0.06 which corresponds to an uncertainty of approximately 1% in the effective track length for a typical alpha energy of 5 - 6 MeV. The effect of the alpha component on the dose rate is given in Table 1.

If the relative concentrations of the radionuclides present is known, an overall correction factor may be calculated. This correction factor will depend on the system used (*a* or *b*, or *k*), on the energy of the alpha particles used to determine the alpha effectiveness, and on whether alpha-thick or alpha-thin targets are used for calibration. Figure 3 is based on the data of figure 2. It presents the factors η and k_{eff}/k_{ref} as previously defined by Aitken and Bowman (1975) and Zimmerman (1971), respectively, as a function of reference energy for thick and thin target calibrations, for the U-238, U-235 and Th-232 chains in equilibrium and for the U-238 chain with 100% radon escape. It should be noted that, although η for a thin-target calibration appears to be independent of the calibration energy used, in practice experimental difficulties, particularly in ensuring a uniformly alpha-thin target for low energy calibration alpha particles (less than 4 MeV), may lead to increased uncertainties and a serious underestimate of alpha effectiveness.

In Table 1, values for η and k_{eff}/k_{ref} for calcite from this study are compared with commonly quoted values for other materials in the literature. Using the *a* or *b* systems, the new correction factors give an estimate of effective alpha dose rate for the complete U-238 chain in calcite that is 6% lower than the best previously available estimate, and for the radon escape case, one that is 5% lower. For the *k* system the revised estimate is 7% lower. The effect on age estimates will depend, however, on the proportion of the environmental dose rate due to alpha irradiation. Note that the values from this study for calcite are not inconsistent with previous estimates for other materials but are more precise, with an uncertainty of less than 2% , as the use of thick rather than thin targets eliminates the uncertainty in all data points due to inadequate knowledge of the slope of the signal *vs* range curve for low energies. Bowman (1976) found values for different materials ranging from 0.84 - 0.95 and Aitken (1985) proposes an average value of 0.90 $\pm$ 0.05 for use with all archaeological dating materials; the error bar partly reflects the variation between materials and partly the difficulty of using thin targets for calibration.

We have also calculated the variation in η and k_{eff}/k_{ref} due to the accumulation of daughter products with time, assuming thorium and its daughters are not initially present, as is usual with speleothem calcite (figure 4). If a systematic error of this magnitude is unacceptable, then the age equation should include the concentrations of the daughter products together with their appropriate correction factors as outlined above.

Parameter	This paper (calcite)	Previous estimates (other materials)	Difference in effective alpha dose estimate
	Equilibrium Case		
η thin	0.85	0.90	- 6%
$(k_{eff}/k_{ref})_{thin}$	0.75	0.80	- 7%
η thick	1.14		
(k_{eff}/k_{ref}) thick	1.34		
	100% Radon Escape		
η thin	0.81	0.86	- 5%
$(k_{eff}/k_{ref})_{thin}$	0.66		
η thick	1.09		
(k_{eff}/k_{ref}) thick	1.18		

Table 1: Comparison of correction factors for calcite (this study) with previous estimates for other materials, for the U-238 chain. η values are average values for several different materials from Aitken and Bowman (1975). The k ratio, taken from Zimmerman (1971), is for Norwegian quartz, an energy of 3.7 MeV being used for k_{eff}.

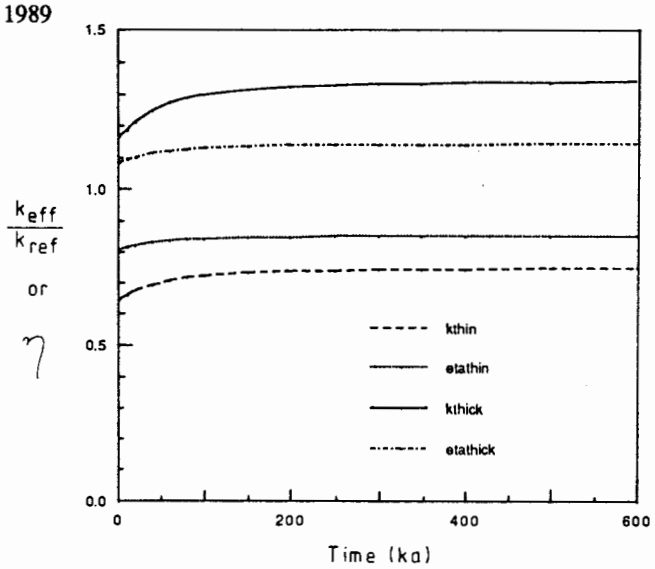

Figure 4: Variation of η with time for the U-238 chain in calcite, assuming initial concentrations of thorium and its daughters to be zero.

As alpha effectiveness is most probably dependent on the stopping power of the material for different energies (and thus on the form of the range *vs* energy curve) and on the saturation properties of the material, it should not be assumed that the above values are definitive for other dating materials. The experimental data from this study is specific to calcite and has smaller uncertainties than the average estimates previously available: we suggest that these values be used for calcite and aragonite (which have the same range *vs* energy curve as calcite), rather than average values.

Acknowledgements

The cooperation and support of the Physics, Chemistry and Geography Departments of the University of Auckland are gratefully acknowledged. In particular, the sustained interest of the Nuclear Physics Group staff, both academic and technical, is invaluable. Our thanks also to Martin Aitken for his helpful comments. The research has been supported by the Geological Survey, Department of Scientific and Industrial Research; one of us, RGL, is grateful for the support of a Postgraduate Scholarship from the University Grants Committee and a Fellowship of the Auckland Federation of University Women.

References

Aitken, M.J., (1985) Thermoluminescence Dating, Academic Press, London.

Aitken, M.J. and Bowman S.G.E., (1975) Thermoluminescent dating: assessment of alpha particle contribution. *Archaeometry*, **17**, 132-138.

Bell, W.T., (1979) Thermoluminescence dating: radiation dose rate data. *Archaeometry*, **21**, 243-245.

Bowman, S.G.E., (1976) Thermoluminescent dating: the evaluation of radiation dosage. D.Phil thesis (unpub) Oxford University.

Bowman, S.G.E. and Huntley, D.J , (1984) A new proposal for the expression of alpha efficiency in TL dating. *Ancient TL*, **2**, 6-11.

Lyons, R.G. Wood, W.B. & Williams, P.W., (1985) Determination of alpha efficiency in speleothem calcite by nuclear accelerator techniques. *ESR dating and dosimetry*, Ionics, Tokyo, 39-48.

Lyons, R.G., (1987) Alpha effectiveness in ESR dating: a preliminary note on energy dependence. *Ancient TL*, **5**(3), 4-6.

Lyons, R.G., (1988) Determination of alpha effectiveness in ESR dating using linear accelerator techniques: methods and energy dependence. *Nuclear Tracks and Radn. Measts.*, **14**(1-2), 275-288.

Nambi, K.S.V. and Aitken, M.J., (1986) Annual dose conversion factors for TL and ESR dating. *Archaeometry*, **28**(2), 202-205.

Zeigler, Z.F., (1977) Helium stopping powers and ranges in all elemental matter. Pergamon Press, New York.

Zimmerman, D.W., (1971) Thermoluminescent dating using fine grains from pottery. *Archaeometry*, **13**, 29-52.

PR Reviewer's comments (M.J. Aitken)

Measurement of alpha effectiveness using thin layers of sample (as is necessary for TL) is made difficult by the tendency of fine grains to agglomerate on deposition, as the authors mention. It therefore reflects well on the experimental work of Zimmerman (1971) and Bowman (1976) that the values they obtained are close to the values now found by the authors using the thick sample technique (as is possible with ESR).

While the effect on dating is barely significant, this work is important not only in substantiating the values of Zimmerman and Bowman but also in giving further confirmation of the validity of the 'TL/ESR per unit track length' model. We look forward to learning the actual *a-, b-, or k-* values determined by the authors for ESR and a definitive comparison with TL values.

Fractional bleaching of potassium feldspar from sediments and its role in equivalent dose determination

J.W.A Dijkmans† and A.G. Wintle‡
†Department of Geography, University of Utrecht, Heidelberglaan 2, 3584 CS Utrecht, The Netherlands.
‡Institute of Earth Studies, University of Wales, Aberystwyth SY23 3DB, UK.

Introduction

Several methods have been developed to determine the equivalent dose (ED) of sediments that might not have been well-bleached during deposition (Berger, 1984; 1985; Berger et al., 1987; Huntley, 1985; Mejdahl, 1985; 1988; Wintle and Huntley, 1980). These all involve a short laboratory bleach which is thought to have less effect on the TL signal than that caused by light exposure prior to deposition. In a preliminary study on the thermoluminescence of eolian sands from the Lutterzand area in the eastern part of The Netherlands, Dijkmans et al. (1988) used the plateau method with additive dose pioneered by Mejdahl (1986; 1988). This method was applied to potassium feldspar grains separated from an eolian sand sample (Younger Cover Sand I). A short plateau from about 340 to 400 °C was obtained using residual signals resulting from 20 to 40 minutes exposure to a SOL 2 sunlamp. Shorter bleaching times resulted in decreasing dose values (D) with increasing glow curve temperatures, whereas longer bleaching times increased those values. The choice of the right bleaching time and therefore of the correct ED was not straightforward.

In a subsequent study twelve samples from the same site were analysed with the automated Risø TL reader using potassium feldspar separates (Dijkmans and Wintle, in prep.). The additive dose-plateau method was found to give poor plateaux in 75% of the cases (fig. 1). Several possible causes of poor plateaux are listed in Appendix A. The calculated dose (D) increased with bleaching time. For at least 50% of the samples no bleaching time could be found which would extend the plateaux to temperatures above 390 °C as recommended by Mejdahl (1988). Therefore another approach was used, based on method (a) of Wintle and Huntley (1980). The basis of this approach is reiterated here and the experimental data obtained for the set of samples were analysed using the approach of Debenham (1985).

Method of ED determination: defining a factor f

For sediments the natural TL-intensity, I, may be separated into an unbleachable part, I_0, (residual value after a long bleach) and a bleachable part, I_d, (TL due to

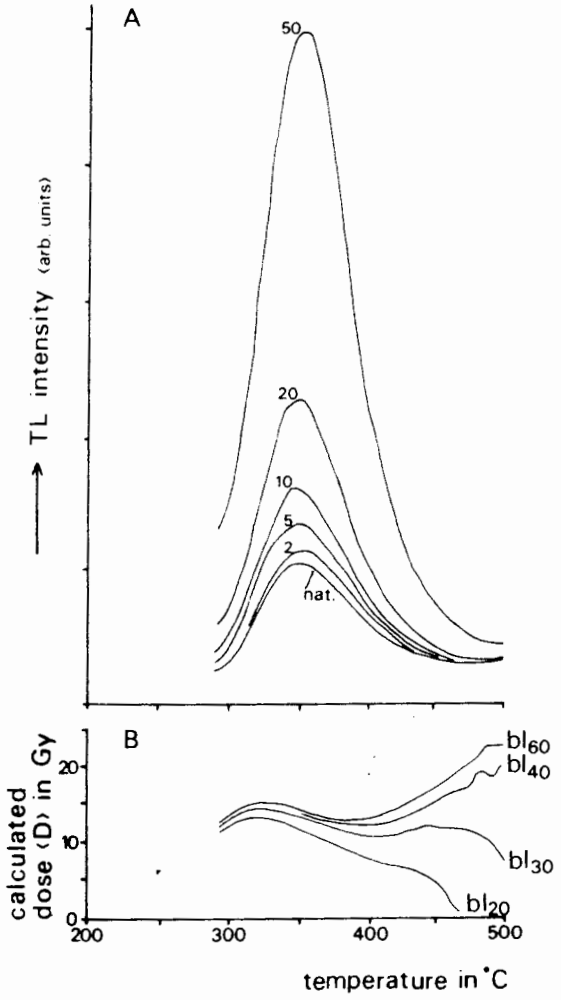

Figure 1
A) Glow curve of natural TL and five glow curves of additive dose, given in minutes of β-irradiation (black body has not been subtracted).
B) Dose (D) versus temperature plots for four different bleaching times (60, 40, 30, and 20 minutes, SOL-2 lamp) for sample L11. The material used is a potassium feldspar separate; preheat 290 °C for 10 sec.; heating rate 10 °C/s; UG-11 filter. Each glow curve represents the mean of four measurements.

radiation dose since deposition) (Wintle and Huntley, 1980):

$$I = I_o + I_d$$

One of the original methods for determination of the ED for deep-sea sediments was introduced by Wintle and Huntley as their method (a). They suggested that the effect of a relatively short exposure to light would result in a bleached signal (I_{bl}):

$$I_{bl} = I_o + f.I_d$$

where f is the fraction of radiation induced TL signal left after that light exposure. The unbleachable component would, of course, be unaffected. Wintle and Huntley (1980) then determined the gamma irradiation D that was needed to replicate the natural TL level. Hence:

$$I = I_o + I_d = I_o + f.I_d + I_D$$

where I_D is the signal due to D. This can be rewritten as

$$I_d = f.I_d + I_D$$

or

$$I_d (1 - f) = I_D$$

Assuming the TL sensitivity (χ) (TL per unit radiation dose) to be a constant, the equivalent dose (ED) can be expressed as

$$ED = \frac{I_d}{\chi}$$

and in a similar way

$$ED = \frac{I_D}{\chi}$$

but $I_D = I_d (1 - f)$, and hence

$$D = \frac{I_d (1 - f)}{\chi}$$

Combining these equations gives

$$D = \frac{I_d}{\chi}(1 - f) = ED(1 - f)$$

or

$$ED = D(1 - f)^{-1} \qquad (1)$$

To determine the ED, f must also be determined experimentally. This is done by measuring the TL (I_{SB}) left in a gamma irradiated sample after the same short bleaching time. This is then compared with the TL for the gamma irradiated sample ($I_{B+\gamma}$). In each case the gamma dose is administered after the sample has been bleached for a long time to reach a base TL level I_B. This may be close to I_o, but is not necessarily identical with it. Hence f is the fraction of gamma induced TL left after the lamp exposure i.e.

$$f = \frac{I_{SB} - I_B}{I_{B+\gamma} - I_B}$$

This procedure is shown schematically in fig. 2, where I_{SB} is presented in four bleaching times (20, 30, 40 and 60 min).

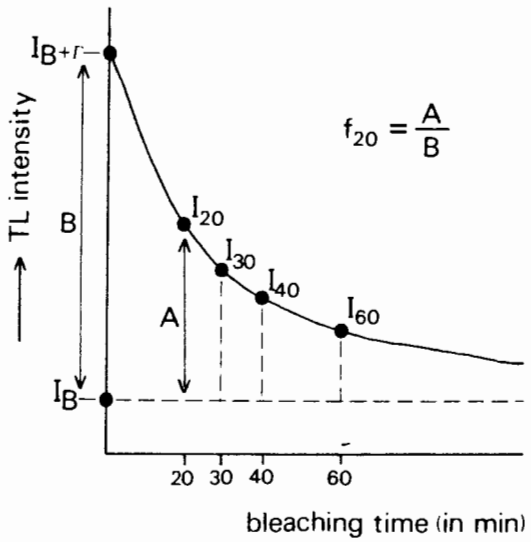

Figure 2
Schematic diagram showing experimental procedure to determine f.

Hence, by using several bleaching times different values of f are obtained. At the same time different values of D will be obtained when the natural TL signal is regenerated after the different bleaching times. However, using equation (1) the same value of ED should be obtained for each data set!

This concept can be taken further, as first suggested by Debenham (1985) for the data he obtained by applying the regeneration method using a 16 hour sunlamp bleach and assuming that $I_o = I_B$. However, laboratory lamp exposures do not usually attain the residual level at deposition (i.e $I_o = I_B$). Hence one can write

$$I_B = I_o + f.I_d$$

but by definition

$$I = I_o + I_d$$

Substituting for I_d:

$$I_B = I_o + f (I - I_o) = f.I + (1 - f) I_o \qquad (2)$$

A plot of I_B versus I would thus have a slope f and an intercept on the y-axis of $(1 - f)I_o$. To demonstrate the fact that f=O Debenham (1985) plotted the value of the residual level, I_B, (in terms of their equivalent dose) after a 16 hour bleach against natural intensities, I, for the same samples. He used fine grained samples from four different sites covering a timespan from 10 to 700

ka and obtained the slopes of this plot at two particular temperatures. f was about 0.05 for the TL at 300 - 310 °C - an indication that 5% of the bleachable TL in the fine grain samples survived the 16 hour sunlamp exposure. The same approach has been applied in the present paper to the 12 eolian sand samples from the Lutterzand.

Experimental procedure and results

Twenty mg weighed samples were measured using a UG-11 filter and employing a pre-heat of 10 seconds at 290 °C as originally recommended by Mejdahl and Winther-Nielsen (1982). Typical glow curves are given in fig. 1A.

Because of the problems with obtaining reproducible plots of dose, D, versus glow curve temperatures (as mentioned earlier), the area beneath the peak, defined by the half height, was used. The procedure differs from that of Wintle and Huntley (1980) in that additive dose was used instead of regeneration. In table 1A values of D are given for four different bleaching times (20, 30, 40, and 60 minutes) for three samples which were examined in detail. It can be seen that D increases systematically with increasing bleaching time.

Further experiments were carried out on these samples in order to calculate the factor f (again using the temperature range between the half peak height), as defined in the previous section. Potassium feldspar separates of the samples were bleached for 5 hours using the SOL 2 lamp. A small part of each sample was measured (I_B in fig. 2) and the rest was given a gamma dose of about 39 Gy. Part of this was measured ($I_{B+\gamma}$ in fig. 2). Subsamples of the irradiated material were exposed to the lamp for 20, 30, 40, and 60 minutes respectively and subsequently measured (fig. 2). For these measurements 20mg samples were used with 4 samples for each data point. Second glow normalization was used to improve the reproducibility.

Glow curves from several stages of the experiment are given for one sample in fig. 3. The values of f are given in table 2 and the resulting values of ED, obtained from putting D and f in equation (1), in table 1B for the three samples.

Besides obtaining f for the integral about the peak, f was also obtained as a function of temperature. f_{20} versus temperature is plotted in fig. 4A for the three samples and for the four bleaching times for one of the samples in fig. 4B. For all three samples the values of f increases with increasing glow curve temperature. This effect was also reported by Wintle and Huntley (1980) who concluded that it was brought about by TL sensitivity changes which occur after exposure to the lamp and to a different extent for different glow curve temperatures. Another reason for the variation of f with temperature could be the particular bleaching response at different temperatures for the lamp used. This may be different from sunlight and requires further investigation.

Table 1. Values of D and ED (in Gy) obtained for three samples for each of four bleaching times. The ED is calculated both by using: B) mean f values for individual samples, C) values of D and f both obtained as a function of temperature, and D) graphically-derived f values as shown in table 2. A preliminary dose rate calibration of 1.64 Gy/min was used.

	Sample L2	Sample L8	Sample L10
A) Dose (D) Obtained by extrapolation to I_B			
D_{20}	12.32	18.40	12.62
D_{30}	12.89	19.50	13.37
D_{40}	13.69	20.37	13.89
D_{60}	14.33	20.93	14.45
mean ED	13.31	19.80	13.58
± 1σ	± 0.88	± 1.10	± 0.78
B) Equivalent dose obtained from D using f values of individual samples.			
ED_{20}	16.02	23.75	16.17
ED_{30}	15.88	23.85	16.74
ED_{40}	15.76	24.11	16.68
ED_{60}	16.09	23.65	17.06
mean ED	15.94	23.84	16.66
± 1σ	± 0.15	± 0.20	± 0.37
C) Equivalent dose obtained from individual values of D and f obtained as a function of temperature (fig. 5)			
ED_{20}	15.61	23.42	16.60
ED_{30}	15.73		
ED_{40}	15.27		
ED_{60}	16.04		
mean ED	15.66		
± 1σ	± 0.32		
D) Equivalent dose obtained from D using graphically derived f values (fig. 6)			
ED_{20}	16.40	24.50	16.79
ED_{30}	16.50	24.97	17.12
ED_{40}	16.88	25.12	17.13
ED_{60}	17.10	24.98	17.24
mean ED	16.72	24.89	17.07
± 1σ	± 0.33	± 0.27	± 0.19

Table 2. f factor for four bleaching times of the three samples. Each data point is represented by four individual measurements and one standard deviation is indicated. f as calculated by linear regression (see fig. 5) using the data of twelve samples are also shown.

Sample	f factor for four bleaching times ± 1σ			
	f_{20}	f_{30}	f_{40}	f_{60}
L2	0.231 ± 0.018	0.188 ± 0.010	0.131 ± 0.018	0.109 ± 0.007
L8	0.225 ± 0.018	0.182 ± 0.016	0.155 ± 0.014	0.115 ± 0.010
L10	0.220 ± 0.017	0.202 ± 0.013	0.167 ± 0.013	0.153 ± 0.011
L1 - L12 (linear regression)	0.249 ± 0.022	0.219 ± 0.037	0.189 ± 0.024	0.162 ± 0.026

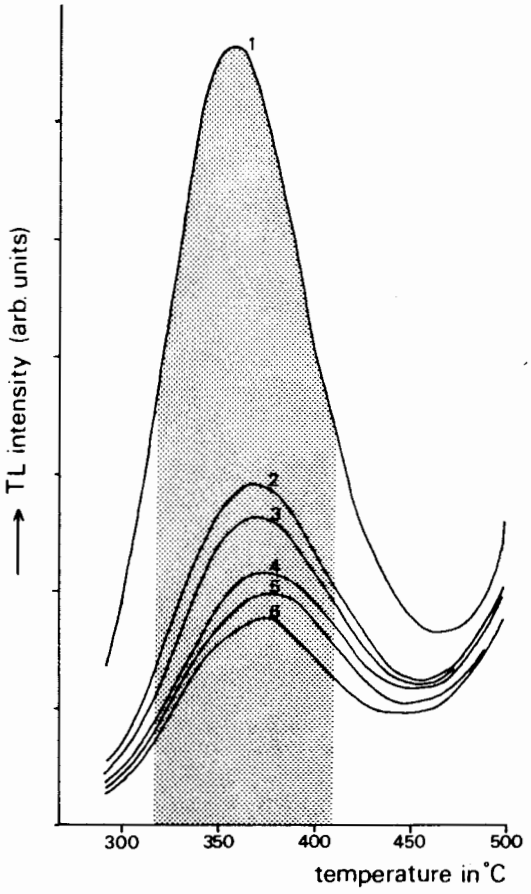

Figure 3
Glow of sample L2 at various stages of the experiment to determine f. 1) $I_B+\gamma$; 2) $I_B+\gamma+bl20$; 3) $I_B+\gamma+bl30$; 4) $I_B+\gamma+bl40$; 5) $I_B+\gamma+bl60$; 6) I_B.. Only the relevant part of the temperature range is shown. The shaded part represents the area between the half peak height. Preheat 290 °C for 10 sec.; heating rate 10 °C/s ; UG-11 filter.

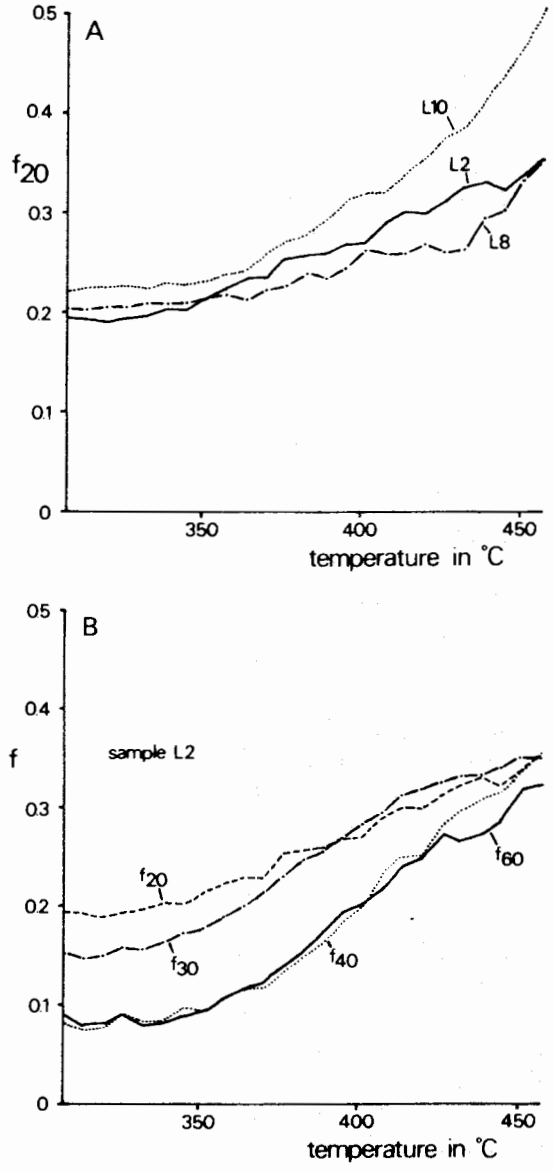

Figure 4.
A: The fraction of gamma induced TL, f, left after 20 minutes exposure to the SOl 2 lamp as a function of temperature for the samples L2, L8 and L10.
B: f as a function of temperature for four different bleaching times (sample L2).

Implication of the factor f for equivalent dose determination

The values of ED obtained for the different bleaching times (as shown in table 1B) are in good agreement with each other for all of the samples used in the experiment. This is exemplified by the low standard deviation of the mean of the four ED values for each sample, as compared with the standard deviation of the mean D (cf. table 1A and B). Moreover there is no systematic increase (or decrease) in ED with bleaching time. For these reasons it can be argued that these values of the ED are the correct values to be used for TL fading of these samples. Combining values of D and f, both obtained as a function of temperature, in equation (1) permits the calculation of ED as a function of temperature. Values of ED are shown for four bleaching times for sample L2 alongside the values of D (fig. 5). The mean values of ED for the temperature range 308-392 °C (half peak height) are given in table 1C, as are the results for the 20 minutes bleach for L8 and L10.

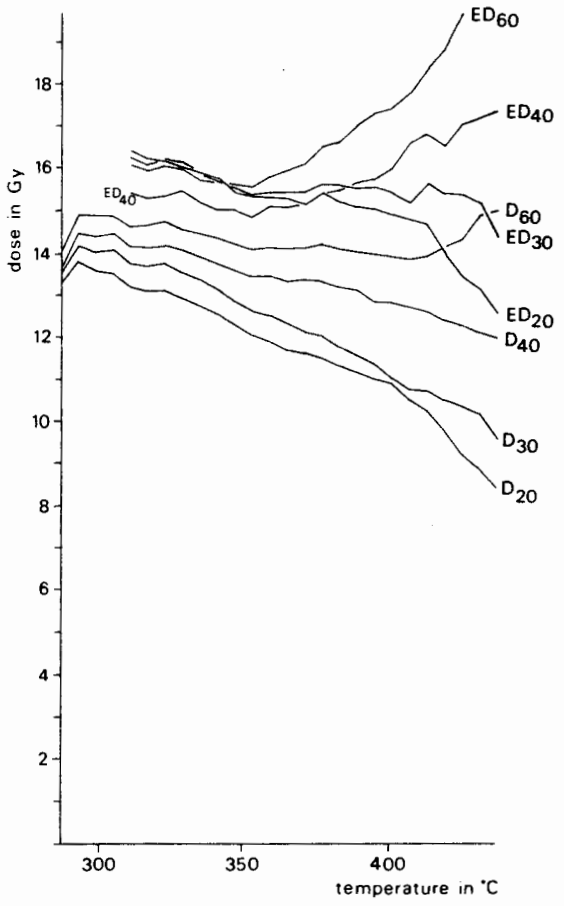

Figure 5. Dose (D) and equivalent dose (ED) versus temperature plot for four different bleaching times (in minutes) of sample L2. The values of the ED are calculated using both D and f obtained as a function of temperature. A preliminary dose rate calibration of 1.64 Gy/min was used.

The data also suggest that none of these bleaching times were sufficient to match the residual level at deposition. This point of view can also be supported by following the same approach as Debenham (1985), which was explained in detail in a previous section. The absolute value of the natural TL after a short bleaching Ibl is given by equation (2): i.e.

$$I_{bl} = I_o + f.I_d$$

and hence

$$I_{bl} = f.I + (1 - f)I_o.$$

Therefore a plot of I_{bl} for a single bleaching time versus the natural TL intensity, I, will have a slope f.

Plots of I_{bl} versus I were obtained for the twelve eolian sand samples from the Lutterzand area which range in age from a few hundred to about fifteen years (fig. 6). Four plots were obtained, one for each bleaching time. Individual data points are given for both the 20 and 60 minutes bleaching times and the straight lines represent linear regression for the four data sets.

The f values obtained in this way can be compared with the f values obtained for the individual samples L2, L8 and L12 as shown in table 2. There is good agreement between the individual values of f and those obtained from fig. 6 (most values agree within one standard deviation) considering no normalization based on absolute TL sensitivity between the twelve different samples was employed. The data imply that potassium feldspars from The Lutterzand area are very similar, in spite of their different ages. This agrees with the geological evidence. They also imply that the values of f obtained from the linear regression using the twelve samples could be applied to the values of D obtained for any eolian sand samples in the Lutterzand area to obtain values of the ED. Using this approach for the three samples used in the experiment, the values of the ED obtained for the different bleaching times (table 1D) also come together without an increasing or decreasing trend with bleaching time. Moreover they are in agreement with the ED values obtained from individual f values (cf. table 1B and 1D). This would justify the use of the graphically derived f values for a group of homogeneous samples in at least a limited geographical area. This approach would involve a considerable reduction in laboratory and analytical work (and sample material) compared with calculating individual f values for each sample to be dated. One must take into consideration that to obtain a reliable value of f from linear regression, a data set is needed with a large variety of natural TL intensities (i.e. use both young and older samples).

Acknowledgements

This study was funded by the EEC collaboration projects: grant ST2P-0204 and ST2J-0085. The authors wish to thank Vagn Mejdahl and Helen Rendell for valuable comments on the manuscript.

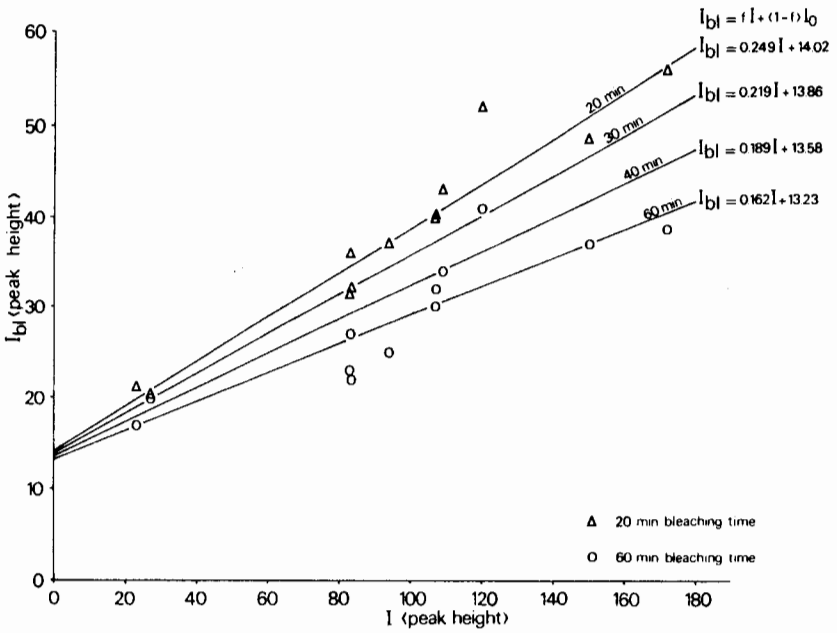

Figure 6. Levels of TL remaining after specific SOL 2 lamp exposure times (I_{bl}) plotted against the natural TL intensities (I), for 12 sand samples from the Lutterzand. Values represent arbitrary units of the peak height at about 360 °C.

References

Berger, G. W. (1984). Thermoluminescence dating studies of glacial silts from Ontario. *Canadian Journal of Earth Sciences*, **21**, 1393-1399.

Berger, G. W. (1985). Thermoluminescence dating studies of rapidly deposited silts from south-central British Columbia. *Canadian Journal of Earth Sciences*, **22**, 704-710.

Berger, G. W., Clague, J. J. and Huntley, D. J. (1987). Thermoluminescence dating applied to glaciolacustrine sediments from Central British Columbia. *Canadian Journal of Earth Sciences*, **24**, 425-434.

Chen, R. Huntley, D. J. and Berger, G. W. (1983). Analysis of thermoluminescence data dominated by second-order kinetics. *Physica Status Solidi (a)*, **79**, 251-261.

Debenham, N. C. (1985). Use of u.v. emissions in TL dating of sediments. *Nuclear Tracks and rad'n Measts.*, **10**, 717-724.

Dijkmans, J. W. A. and Wintle, A. G. (in prep.) Thermoluminescence dating of cover and drift sand from the eastern part of The Netherlands.

Dijkmans, J. W. A., Wintle, A. G. and Mejdahl, V. (1988). Some thermoluminescence properties and dating of eolian sands from The Netherlands. *Quaternary Science Reviews*, **7**, 349-355.

Huntley, D. J. (1985). On the zeroing of the thermoluminescence of sediments. *Physics and chemistry of minerals*, **12**, 122-127.

Levy, P. W. (1982). Thermoluminescence and optical bleaching in minerals exhibiting second order kinetics and other charge retrapping characteristics. *PACT J.*, **6**, 224-242.

Mejdahl, V. (1985). Thermoluminescence dating of partially bleached sediments. *Nuclear Tracks and Rad'n Measts*, **10**, 711-715.

Mejdahl, V. (1986). Thermoluminescence dating of sediments. *Radiation Protection Dosimetry*, **17**, 219-227.

Mejdahl, V. (1988). The plateau method for dating partially bleached sediments by thermoluminescence. *Quaternary Science Reviews*, **7**, 347-348.

Mejdahl, V. and Winther-Nielsen, M. (1982). TL dating based on feldspar inclusions. *PACT J*, **6**, 426-437.

Wintle, A. G. and Huntley, D. J. (1980). Thermoluminescence dating of ocean sediments. *Canadian Journal of Earth Sciences*, **17**, 348-360.

Appendix A: Possible causes of poor plateaux in the additive dose method

1. Non-linear growth of TL signal - not found to be a problem for these samples when linear and exponential fits were compared.
2. At higher glow curve temperatures the TL signals are smaller because of lower sensitivity (fig. 1), and hence there is a greater potential for error.
3. Second order kinetic behaviour causing peak shifts resulting in supralinearity (Chen et al., 1983; Levy, 1982).
4. Inappropriate choice of light source (SOL-2 lamp) as proposed by Mejdahl (1988), but this is unlikely in our experience (Dijkmans et al., 1988, fig. 7).

PR. Reviewer's comments (Helen Rendell)

This paper sets out to explore the logical implications of Wintle and Huntley's (1980) method (a) for ED determination. In this method both D, the gamma dose required to match exactly the natural TL, and f, the fraction of radiation induced TL left after a short exposure to light, are determined for a range of glow-curve temperatures. Some of the underlying assumptions, notably that TL sensitivity to dose will be unaffected by bleaching, are inevitably problematic. One might also suspect that the value of f obtained will be a function of both bleaching spectrum and the wavelength range of TL emissions monitored. Nevertheless the results quoted should encourage other workers to explore this method of ED determination.

One small point on experimental method: the heating rate claimed (10 °C/s). Am I alone in being worried by the implications of such (apparently) rapid heating? Perhaps a plot of $\ln(T^{*2}/\beta)$ against $1/T^*$ for this material would help to remove this source of concern!

Ancient TL, Volume 7 No.1 1989

A note on overcounting in alpha-counters and its elimination

L.Zöller & E.Pernicka, Max-Planck-Institut für Kernphysik, Heidelberg, West Germany.

Summary

Overcounting in alpha-counters is found to depend on the grain size distribution of the sample rather than from radon escape. The U- and Th- activity of several sediments was measured by alpha-counting and neutron activation analysis. Overcounting was detected in samples with a considerable grain size fraction larger than 20 μm. Further decrease of the grain size by grinding resulted in good agreement of the alpha dose derived from alpha-counting with the alpha dose calculated from neutron activation data. Concentrations of Th- and K in loess samples increase with decreasing grain size of the unpowdered sample, whereas the U-distribution appears to be more homogenous.

Introduction

Overcounting in alpha-counters has been observed in numerous cases. The most striking example is the "Hong Kong sand" with a count rate of ca. 160% higher than expected from concentrations of U and Th, which were determined by neutron activation analysis (NAA) (cf. Pernicka & Wagner, 1982). In our laboratory, α-overcounting proved to be a serious problem for TL-dating of some loess samples from Rotenberg and Nussloch, south of Heidelberg, West Germany (Zöller et al., 1988). The α-dose calculated from NAA data was up to about 30% lower than the values obtained from α-counting. If the β- and γ-dose rates are derived from the α-count rate, the error of TL age determination is even larger. There was no systematic difference between the count rates of sealed and unsealed samples, which is usually taken as indication of radon escape from the sample. In some cases, the sealed count rate was even slightly lower than the unsealed one. This may be explained by electrostatic attraction of radon atoms to the perspex holder immediately after filling in the ground sample. After some hours or days of delay this effect disappears. We observed this effect in many other loess samples, too, and it may also be the cause for some low sealed/unsealed count-rate ratios published by Wintle (1987) and Juvignè & Wintle (1988). Since radon escape obviously cannot account for α-overcounting satisfactorily, we looked for other possible explanations.

Sedimentological characteristics of the loess samples

The loesses from the sections near Rotenberg (RO) and Nussloch (NU) south of Heidelberg are characterized by different grain-size distributions with a larger median diameter compared with "normal" German loesses. Most of them can be classified as sandy loess. This is readily explained by a short transportation distance from the source area, namely the large plain of the Upper Rhine valley, which was drained by a braided river system during the pleniglacial (Bente & Löscher, 1987). In some parts of the Middle Würmian (=lower pleniglacial) loess sequences even aeolian sands occur. The mean clay content of the loesses (<10%) is unusually low, while sand contents often exceed 10%. The maximum of the grain size distribution lies within the middle and coarse silt fractions (cf. fig.1, after Bente & Löscher, 1987). However, in paleosols decomposition of mineral grains due to soil formation results in higher clay contents at the expense of sand and coarse silt. In the case of para-brownearths, pores of the Bt-horizon are coated with clay (NU-4). In these samples overcounting is less pronounced.

Experimental details

Two scintillation α–counters (Littlemore Eng. Co.) were used for thick source α– counting. Round screens with a diameter of 42 mm and a coating of ZnS were covered with ca. 1 mm of loess. Both α-counters were calibrated with two standards, whose U and Th contents have been determined by NAA. Secular equilibrium was confirmed by α- and γ-spectrometry. These standards were: O-110 (obsidian, grain size <50 μm, expected count-rate 4.54 ± 0.10 min^{-1}), and TONY (sedimentary clay, expected count-rate 1.11 ± 0.03 min^{-1}). Most samples were counted on both counters (1000 counts minimum). After a first count the sample holders were sealed and the α- activity counted again after a delay of several days. Originally the loess aggregates were only slightly crushed using an agate mortar without breaking up single grains. The α-counting procedure was repeated after powdering the samples for 15 min in an agate ball mill. U and Th have been determined by instrumental neutron activation (Pernicka & Wagner, 1982). Then alpha-dose-rates were calculated from NAA data using conversion factors calculated by Nambi & Aitken (1986).

Results

Count-rates of selected samples, together with concentrations of U and Th, are listed in table 1. Overcounting is most prominent with those loess samples which consist essentially of middle and coarse silt with relatively high sand and low clay contents (NU- and RO-series, except for NU-4 from a strongly altered soil horizon).

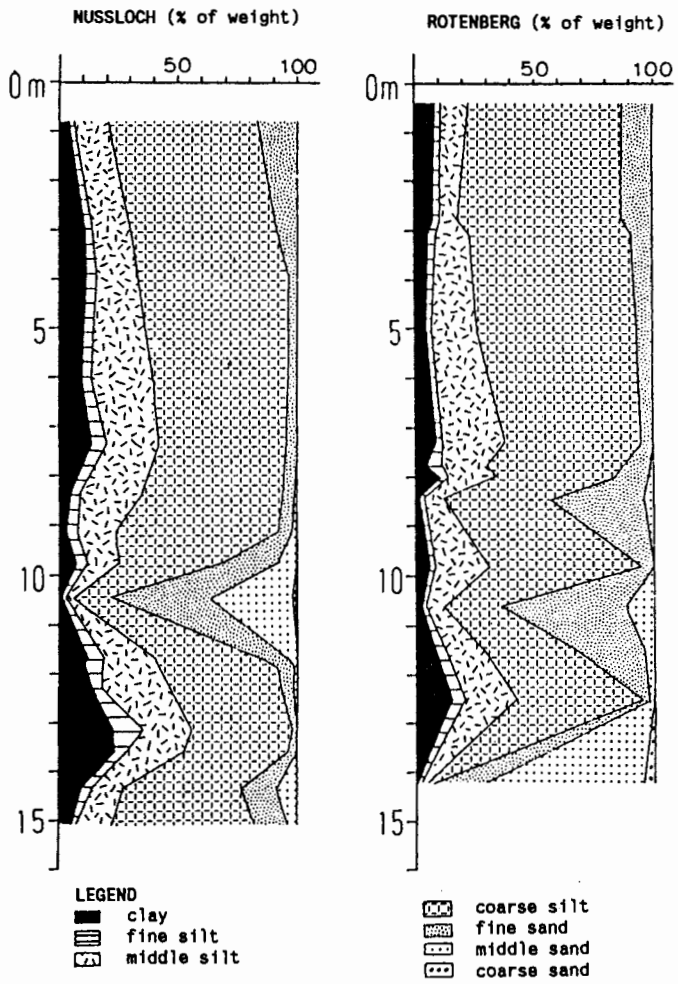

Figure 1 Grain size distributions in the loess sections of Nussloch and Rotenberg south of Heidelberg, W-Germany. Except for sandy layers, the coarse silt fraction (20-63 µm) is the main grain size fraction of these loesses. The high clay content at a depth of 12.5 to 14 m in the Nussloch section is due to interglacial weathering and soil formation.

Samples of "normal" fine grained loess (KAE-series, RD-8) from the Kaerlich pit and from Rheindahlen do not exhibit overcounting; in the case of KAE-4, the α–count-rate is even 10.5% lower than expected from NAA data, assuming secular equilibrium. In a sandy silt from tidal deposits (WA-4) from the Wacken pit α–overcounting amounts to 49%, whereas for powdered quartz grains from the same exposure (WA-2) the results are in excellent agreement with NAA despite their extremely low α–activity. Table 2 demonstrates the effect of powdering on the α–count-rate. The count-rates of coarse grained samples of the RO-series are about 10-46% higher than the count-rates of the same samples after they have been powdered. The maximum value for overcounting was found for the "Hong Kong sand" (see Pernicka & Wagner, 1982). Even this sample after grinding to a grain size <20 µm comes to an α–count-rate within 5% of the expected count-rate from U and Th contents. On the other hand α–count-rates of samples from "normal" grained loesses (SO-series) from the Bad Soden pit are much less affected by powdering. Overcounting ranges between 2 and 15% only. In the case of sample RO-8p (powdered) , the α–dose-rate derived from the α–count-rate agrees excellently with the α–dose-rate calculated from NAA data. This sample was also analyzed by α–spectrometry and found to be in secular equilibrium.

Obviously it is not necessary to immobilize radon for α–counting using a resin (Murray, 1982) or a glassy melt (Jensen & Prescott, 1983, Huntley et al.,1986,). Therefore it seems that overcounting is not primarily caused by diffusion of radon to the ZnS screen but by the gaps filled with air, which result when the grain size of the sample is of the same order as the range of the α–particles in the solid (ca. 25 µm), and when there are few smaller grains to fill the gaps.

In order to test this hypothesis, we separated different grain size fractions of the sample RO-8 with equivalent diameters of <2 µm, 2 - 6.3 µm, 6.3 - 20 µm, and 20-63 µm by sedimentation in Atterberg glass cylinders. In these four grain size fractions U-, Th-, and K- concentrations were measured by NAA and compared with their α–activities. The results listed in table 3 show a significant increase of Th- and K-concentrations with decreasing grain size, whereas U-concentrations are relatively constant (NAA data). The slightly higher U-concentration in the fraction >20 µm may be due to zircon grains, because the maximum zircon-concentration in sediments is normally observed within the fine sand fraction, 63-200 µm. The α–dose-rates calculated from NAA data and from the α–count-rates of the four grain size fractions agree within 10% only after grinding. The agreement is less without grinding. These results confirm that:

i) within the range of α-particles there exists an inhomogeneous distribution of radioactivity in loess,
ii) radioactivity in loess is concentrated in the finest grain size fractions, and
iii) overcounting is probably dominated by a geometric effect due to large grain sizes, because the air filling the gaps between large grains has a significantly lower stopping power for α–particles. Therefore in many cases overcounting can not be detected by counting the sample sealed and unsealed.

Conclusions

If α–counting is used to estimate dose-rates of U- and Th-decay chains for TL dating, significant

underestimates of TL ages may result from α–overcounting, which may remain undetected by the usual practice of counting a sample with the container open and closed. For example, 60.5% of the effective dose-rate derives from U- and Th-decay chains in loess, if typical values (3 ppm U, 10 ppm Th, 1.5% K, cosmic dose-rate = 0.15 Gy/ka, *a* value = 0.09, and δ=1,15 = moist weight/dry weight) are assumed. Loesses of local origin, i.e. with short transport distances, frequently contain coarser grains and hence α–overcounting can be expected for unpowdered sample aliquots. These problems can be overcome by simple powdering of the loess before α–counting. Melting of the sample as was suggested by Huntley et al. (1986) does not seem to be necessary in the case of loess.

Acknowledgements

We thank M. Aitken and A. Wintle for some helpful comments.

References

Bente, B. & Löscher, M. (1987): Sediment-ologische, pedologische und stratigraphische Untersuchungen an Lössen südlich Heidelberg. *G öttinger Geographische Abhandlungen*, 84:9-17.

Huntley, D., Nissen. M.K., Thomas, J., & Calvert, S.E. (1986): An improved alpha scintillation counting method for determination of Th, U, Ra-226, Th-230 excess, and Pa-231 excess in marine sediments. *Can. J. Earth Sci.*, **23**, 959-966.

Jensen, H.E. & Prescott, J.R. (1983): The thick-source alpha particle counting technique: comparison with other techniques and solutions to the problem of overcounting.. *PACT Journal*, **9**, 25-35.

Juvignè, E.H. & Wintle, A.G. (1988): A New Chronostratigraphy of the Late Weichselian Loess Units in Middle Europe based on Thermo-luminescence Dating. *Eiszeitalter u. Gegenwart*, **38**, 94-105.

Murray, A.S. (1982): Discrepancies in the alpha counting of known activity samples.- *PACT Journal*, **6**, 53-60.

Nambi, K.S.V. & Aitken, M. (1986): Annual dose convertion factors for TL and ESR dating.- *Archaeometry*, **28**, 202-205.

Pernicka, E. & Wagner, G.A. (1982): Radioactive equilibrium and dose-rate determ ination in TL dating.- *PACT Journal*, **6**, 132-144.

Wintle, A.G. (1987): Thermoluminescence dating of loess at Rocourt, Belgium. *Geologie en Mijnbouw*, **66**, 35-42.

Zöller, L., Stremme, H.E., & Wagner, G.A. (1988): Thermolumineszenz-Datierung an Lößβ-Paläoboden-Sequenzen von Nieder-, Mittel- und Oberrhein/ Bundesrepublik Deutschland.*Chemical Geology* (Isot. Geosc. Sect.), **73**, 39-62.

PI. Reviewer's comments (Martin Aitken)

It is now nearly 10 years since strong evidence for overcounting was reported at the 1980 Specialist Seminar (Murray 1982; Pernicka and Wagner, 1982). That thick source alpha counting continues in extensive routine use nevertheless is indicative of its high sensitivity, its convenience, and its direct relevance to the evaluation of alpha dose-rate. The above authors reported the effect primarily in respect of pottery though it was also evident in soil and sand. The present authors report that whereas in some samples of 'normal' fine-grains loess the effect was absent, in some coarser loess the overcounting was strong; they conclude that by powdering the sample (following Jensen and Prescott, 1983) the effect can be avoided though giving direct comparison with neutron activation only for 3 samples: RO8, WA2 and HS. Overcounting was also reported recently by Wintle and Dijkmans (1988) in respect of some Dutch sands; although they too found the effect to be substantially reduced by crushing, the crushed count-rate remained substantially in excess of that predicted by gamma spectrometry (by between 20% and 40% for their 6 samples measured). On the face of it, this suggests that crushing is effective in some samples but not in others. However it must be borne in mind that unless the state of radioactive equilibrium has been measured, any comparison with prediction is far from definitive. Z & P state that RO8 has been found to be in equilibrium but there is no information given on the Dutch sands.

The finding that the potassium and thorium contents are substantially higher in the O - 2 μm fraction of sample RO8 parallels that for a sample of pottery as reported by Murray (1982a), who refers to a similar finding by Scott (1968) in respect of river sediment. I agree that this unhomogeneity in radioactivity is likely to contribute to overcounting but I think that radon emanation may be of major importance too. Unfortunately the sealed/unsealed test for emanation does not appear to be working in the present work and so there is no reliable evidence as to whether these samples emanate. In tables 1 - 3 the sealed count-rate is never more than 10% high than the unsealed, except in one instance (the O - 2 μm fraction of RO8). However the samples include the notorious Hong Kong sand (HS) for which strong emanation is well attested: Pernicka and Wagner (1982) report a radon escape of 21%; at Oxford, Huxtable observes a sealed/unsealed ratio 1.3 - 1.4 depending on the degree of powdering. The authors find a ratio of only 1.05.

In any quantitative assessment of the degree of overcounting, the basis used for calibration is relevant. The present authors mention use of two standards for calibration but for both these the observed count-rate is in excess of that predicted by neutron activated by 8% and 6%. There is now a wide range of geological standards available (mostly as fine powder) and it would seem sense for all alpha counting laboratories to quote the value obtained for at least one of these when publishing; results for some of these standards have been given, for instance, by Goedicke (1983), Aitken (1985) and Huntley et al (1986). The Oxford labaratory still has limited supplies available for send-out, of Sand 105A (10.2ppm U; pitchblende in silica) and Sand 109 (104 ppm Th; 3.7 ppm U; monazite in silica) from the New Brunswick Laboratory.

Additional references

Aitken, M.J. (1985) *Thermoluminescence Dating*, Academic Press

Goedicke C. (1983) Dose-rate determination by alpha counting, *PACT J.*, **9**, 19-23

Murray, A. S. (1982a) Stability of radioisotope concentrations and their dependence on grain size, *PACT J.*, **6**, 216-223.

Wintle, A. G. and Dijkmans, J. W. A. (1988) Dose rate comparisons of sands for thermoluminescence dating, *Ancient TL*, **6(1)**, 15-17.

Neutron activation analysis				alpha counter II			
	U (ppm)	Th (ppm)	Dα (Gy/ka)	count-rate unsealed	Dα	count-rate sealed	Dα
NU1	2.9	9.6	12.56	0.766	16.47	0.788	16.94
NU2	2.9	10.6	13.19	0.708	15.22	0.699	15.03
NU3	3.5	11.0	14.78	0.806	17.33	-	-
NU4	3.3	14.9	16.82	0.829	17.82	0.823	17.69
NU5	2.7	8.7	11.54	0.774	16.64	-	-
RO1	2.9	8.2	11.67	0.734	15.78	-	-
RO8	2.8	9.5	12.27	0.719	15.46	-	-
KAE1	3.2	12.0	14.75	0.626	13.46	0.679	14.60
KAE2	3.4	11.5	14.88	0.661	14.21	0.695	14.94
KAE4	3.5	15.0	17.33	0.722	15.52	0.680	14.62
RD8	3.3	12.5	15.29	0.670	14.41	-	-
WA4	1.58	4.82	6.58	0.456	9.80	-	-
WA2p	0.09	0.17	0.31	0.0127	0.27	-	-
HS	3.78	16.4	18.84	2.220	47.73	2.33	49.63
Standards (Errors are 3% for Th in both standards and 3% for U in O-110 and 5% for U in TONY.)							
O110	28.3	54.5	97.52	-	-	4.916	105.7
TONY	5.79	17.15	23.80	-	-	1.179	25.35

Table 1 Comparison of alpha count-rates and neutron activation analysis data (α dose-rates in Gy/ka, α-count-rates in min^{-1} on 42 mm diameter ZnS screen). NU=Nussloch loess or soil, RO=Rotenberg loess or soil, KAE=Kaerlich loess or soil, RD =Rheindahlen decalcified loess, WA4=Wacken, sandy silt, WA2=Wacken quartz sand, HS=Hong Kong sand, p=powdered in agate mill.

Sample	alpha counter I				alpha counter II			
	unsealed		sealed		unsealed		sealed	
	c - r	Dα	c - r	Dα	c - r	Dα	c - r	Dα
RO2	-	-	-	-	0.836	17.97		
RO2p	0.556	11.95	0.541	11.84	0.577	12.29	0.557	11.86
RO3	-	-	-	-	0.673	14.47	-	-
RO3p	0.606	13.03	-	-	0.611	13.14	-	-
RO6	-	-	-	-	0.798	17.16		
RO6p	0.583	12.54	0.487?	10.46?	0.563	12.11	0.571	12.16
RO7	-	-	-	-	0.757	16.28	0.707	15.20
RO7p	0.581	12.49	-	-	0.557	11.98	0.548	11.79
RO8	0.667	14.34	0.680	14.49	0.734	15.78	-	-
RO8p	0.585	12.58	0.568	12.10	-	-	0.590	12.57
SO2	-	-	-	-	0.74	15.90	-	-
SO2p	0.665	14.30	0.692	14.88	-	-	0.703	15.11
SO3	-	-	-	-	0.706	15.18	0.687	14.77
SO3p	0.571	12.28	0.556	12.17	-	-	0 599	12.88
SO4	-	-	-	-	0.653	14.04	-	-
SO4p	0.602	12.94	0.578	12.43	0.642	13.80	0.697	14.99
HS	-	-	-	-	2.220	47.73	2.330	49.63
HSp	-	-	-	-	0.984	20.96	-	-

Table 2 Effect of powdering of loess samples on the α-count-rates ("p" after sample code means powdered in an agate mill). SO=Bad Soden loess or soil.

fraction (μm)	NAA U (ppm)	Th (ppm)	K (%)	Dα (Gy/ka)	αcount rate (I) unsealed	Dα (Gy/ka)	sealed	Dα (Gy/ka)
0-2	2.78	22.8	2.81	20.69	0.949	20.40	1.045	22.47
2-6.3	2.34	12.7	2.61	13.28	0.732	15.74	0.726	15.61
6.3-20	2.79	7.8	1.59	11.17	0.590	12.69	-	-
6.3-20p					0.500	10.75	-	-
20-63	3.00	7.8	0.93	11.64	0.703	15.11	-	-
20-63p					0.605	13.01	-	-

Table 3 Neutron activation analysis data and alpha-count-rates from different grain size fractions (clay to coarse silt fraction) of sample RO-8 (p=powdered fraction).

110 °C TL peak records the ancient heat treatment of flint

H.Y. Göksu, A. Weiser and D.F. Regulla
Institüt für Strahlenschutz, Gesellschaft fur Strahlen- und Umweltforschung München, D-8042 Neuherberg, Federal Republic of Germany.

In recent years there has been an increased interest among archaeologists in the firing temperature of flints for two reasons. Firstly, in connection with the practise of heating flints before shaping them into tools in prehistoric times. Secondly, for those flints which were heated, there is the question of whether the heating temperature was adequate for zeroing the geological signal in order to obtain reliable ages by the thermoluminescence dating method. It has been found that the thermally activated sensitivity change of the 110 °C thermoluminescence (TL) peak of flints can be used to provide a simple, reliable test for the temperature determination of ancient heat treatment. The method has several advantages over other methods developed earlier. It does not require the source material for comparison. It is simple and quick, and TL dating laboratories may use it without the need for extra equipment.

In early work the most common test was based on the examination of the visual appearance. The change in colour, vitreous lustre, cracks and potlids are often taken as evidence of heat treatment. Many forms of flint exhibit these characteristics. However, they are not always clearly visible and they may even result from non-thermal effects like frost and weathering.
More sophisticated techniques have recently been developed. Weymouth and Mandeville (1975) have studied heat treated cherts by x-ray diffraction and have observed broadening of diffraction lines. Robins et al. (1978, 1981) and Wieser et al. (1986) used electron spin resonance spectroscopy for detecting former heat treatment in flint. A number of signals are reported that are associated and could be altered by the heat treatment in the temperature range 200 - 800 °C. Johnes et al. (1979) studied the effect of heat treatment on the Mössbauer spectrum. It was shown that iron compounds which are present as impurities in flints are altered by heat treatment above 275 °C and this can be revealed by the iron-57 spectrum.
All of these methods require additional equipment and facilities which may not be easily accessible by TL dating laboratories. Some of the above mentioned methods require geologically identical unheated material in order to be certain about the heating temperature. Apart from these, two more methods were developed which make use of the TL properties. The first method was developed by Melcher and Zimmerman (1977). For samples which were heated at some point during the last 8000 years, the equivalent radiation dose was at least 100 times less than that observed for the raw flint, in which the TL signal was in saturation. By comparing the equivalent dose of a particular sample with the dose needed to saturate the TL signal, it was possible to determine heating temperatures. However, this method has certain drawbacks because for certain types of flint the TL signal saturates at relatively low levels of doses (20 Gy) which are comparable with archaeological doses (Göksu, 1973). Furthermore, possible partial annealing of the geological thermoluminscence may cause further difficulties in the interpretation of the results.
The second TL method, developed by Valladas (1983), is based on the thermally activated sensitivity change of the 380 °C TL peak of flint. However, if the archaeological heat treatment was below 500 °C, this method is not sensitive enough to indicate the firing temperature.

Results

In this work we have observed that the sensitivity of the 110 °C peak increases in a similar fashion to the 380 °C TL peak and that it can be used for the assessment of archaeological heat treatment. In this experiment, 5 flints of different geological origins from the eastern part of Turkey were used. The samples were broken into small pieces and each piece was heated to different temperatures from 200 °C to 700 °C for 1 hour. One was kept unheated for control measurement. After grinding and sieving, grains between 75 and 175 microns were selected, washed with acetone to eliminate the very fine grains sticking to the surface. Then 6 mg aliquots were spread evenly on aluminium trays and irradiated with a Sr90/Yr90 beta source with a dose of 1.40 Gy. The TL area under the 110 °C peak was recorded between 50-150 °C using a Harshaw 2000 B automatic integrating picoammeter, similar to that used in TL dosimetry. The sample was heated on a graphite heating planchet in a dry nitrogen atmosphere, using a constant heating rate of 8 °C/sec. The TL intensity of the 110 °C peak increased approximately by a factor of 20 after 700 °C preheating (Figure 1).

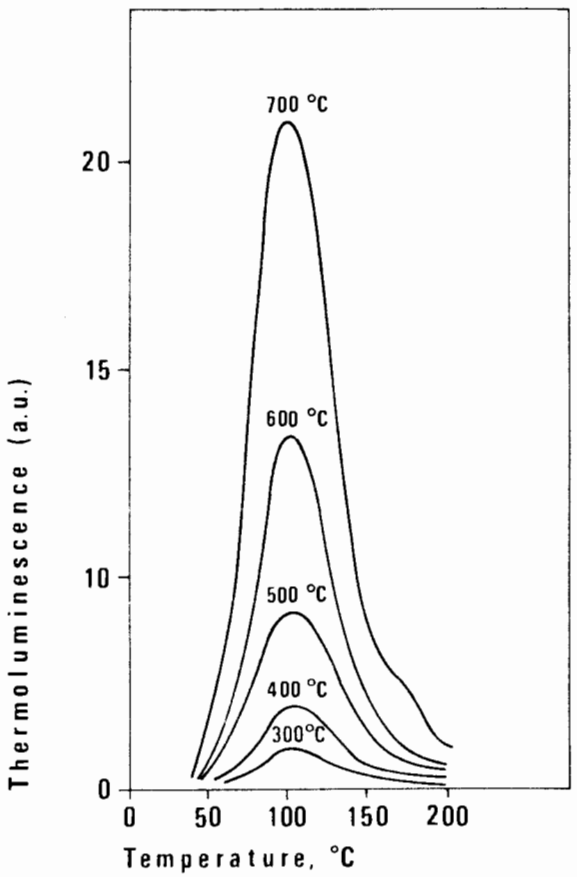

Figure 1 *Thermally activated sensitivity change of the 110 °C TL peak. Aliquots of a geological sample exposed to the same radiation dose after they had been heated to various temperatures for one hour.*

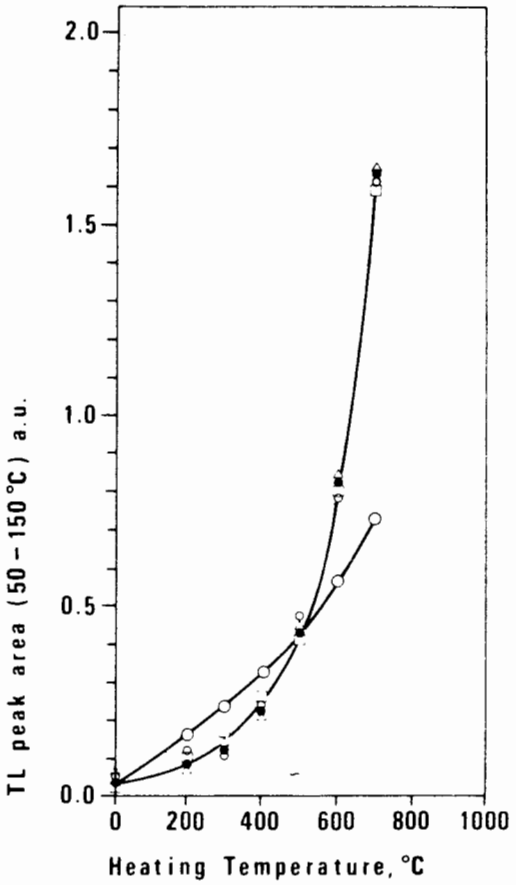

Figure 2 *Geological flints; Annealing temperatures versus TL glow area (50 - 150 °C) for samples exposed to the same test dose. The samples originated from the following sites. O - Hasek Höyük(red), • - Hasek Höyük (grey), ❑ -Degirmentepe, Δ - Tepecik, o - unknown source.*

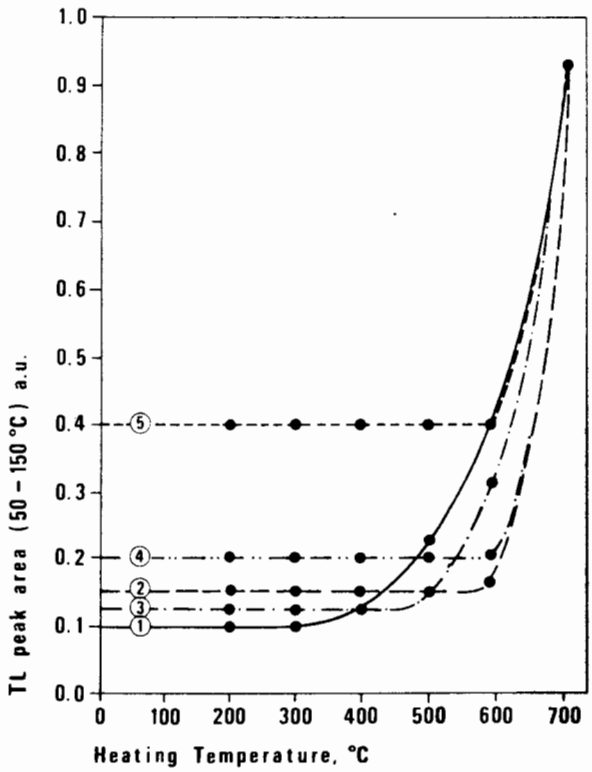

Figure 3
Flints from the burned layers of Hasek Hoyuk were found to be heated to different temperatures. From the marked change of the slope of the sensitivity curves the archaeological heating temperatures are determined.

Figure 2 illustrates the thermally activated sensitivity change of the 110 °C peak for five different geological samples from different origins. As can be seen, under laboratory heat treatment, four samples have a very similar increase in TL, while one sample behaved differently.

To test the method, samples from the burned layers of Hasek Hoyuk are used. To simplify the test further, fine grains were deposited on 6mm diameter stainless steel discs and 8 discs were prepared from each sample. The sensitivity of 110 °C peak was measured by exposing the samples to 1.40 Gy after they had been annealed at different temperatures. From the rise of the sensitivity curves the heating temperatures were determined. As can be seen in figure 3., sample 1 was heated to 400 °C, sample 3 below 500 °C, and the other three samples were heated above 500 °C.

Conclusion

The use of the 110 °C peak has several advantages over other methods. The 110 °C peak does not exist in natural samples and can only be regenerated after the administration of radiation doses; it therefore offers the possibility of detecting previous annealing below 400 °C. The 110 °C peak is less prone to spurious signals which may arise due to grinding or heating, so that even small changes in sensitivity can be detected. Additionally, the TL sensitivity of the 110 °C peak to radiation is high enough to be observed with low doses (below 1Gy); therefore the irradiations and measurements are shorter than when the high temperature peak is used.

Further studies on the effect of duration of annealing and cooling are needed in order to understand better the effect of thermally induced sensitivity change of the 110 °C TL peak in flint.

Acknowledgements

We wish to thank Dr R. H. Behm-Blanke, Dr K. L. Weiner and A. M. Ozer for providing archaeological and geological samples used in this experiment.

References

Göksu, H. Y. (1973) Thermoluminscence dating of burned flints. PhD Thesis, Birmingham University (UK).

Johnes, C. H. W., Dombsky, M. and Skinner, A. F. (1979) Effect of heat treatment on the iron-57 Mössbauer spectrum. *J. Phys Colloq.*, 2, 46.

Melcher, C. L. and Zimmerman, D. W. (1977) TL determination of heat treatment of chert artefacts. *Science*, **197**, 1359-1362.

Robins, G. V., Seeley, N. J., McNeil D. A. C. and Symons, M. C. R. (1978) Identification of ancient heat treatment in flint artefacts by ESR spectroscopy. *Nature*, **276**, 703-704.

Robins, G. V., Seeley, N. J., Symons, M. C. R and McNeil, D. A. C. (1981) Manganese II as an indicator of ancient heat treatment in flint. *Archaeometry*, **23**, 103-107.

Valladas, H. (1983) Estimation de la temperature de chauffe de silex prehistoriques par leur thermoluminscence. *Paris Comptes Rendus de l'Academie des Sciences*, **296**, 993-996.

Weymouth, T. W. and Mandeville, M. (1975) An x-ray diffraction study of heat treated cherts and its archaeological implications. *Archaeometry*, **17**, 61-67

Wieser, A., Göksu, H. Y. and Regulla, D. F. (1986) The ESR spectrum as an indicator of the archaeological heating temperature of flints. *Proc. of 1st International Conference on Prehistoric Flint Mining and Lithic Raw Material Identification in the Carpathian Basin, Budapest-Sumeg, 20-22 May 1986*, 175-182.

PR Reviewer's comments (Steve Sutton)

Pre-dose dating of quartz is complicated by natural activation of the 110 °C peak sensitivity under ambient conditions. Exploiting this effect to estimate the degree of heat treatment experienced by flints is an interesting idea. the basic premise is that the activation curve of an ancient heat treated flint will show a plateau until the heating temperature is reached at which point additional sensitization occurs. the reliability and accuracy of this method remain to be demonstrated. Much work has been done in attempting to understand sensitization phenomena in quartz and analagous experiments on flint need to be conducted, as suggested by the authors. Such work should include studies of grinding effects, test dose activation and reproducibility within individual specimens, all of which are likely to be different for each flint. Most crucial are simulation experiments, ie if one preheats a geologic (naturally unheated) flint in the laboratory to some known temperature and then applies this technique, is the correct result obtained? The stability of flint sensitivity over long timescales should also be explored.

Reply:

Our experiments were primarily based on simulation, ie geological samples were heated in the laboratory (first five samples). Therefore correct results were obtained. However, I agree with the Reviewer that the method has to be tested for long term stability of the sensitivity. We have not observed any effect of grinding on 110 °C peak in flint. Therefore we believe this is the main advantage over the method developed by Dr H. Valladas. Concerning the duration of heating, our recent experiments had showed that the effect is the same whether they are heated for 15 mins or one hour.

Ancient TL, Volume 7 No.1 1989

The use of LEDs as an excitation source for photoluminescence dating of sediments

N.R.J Poolton and I.K. Bailiff
Joint Archaeology- Geography TL Sediment Dating Laboratory, Woodside Building, University of Durham, South Road, Durham, DH1 3LE.

In this note we describe the configuration and performance of a simple and low-cost photo-excitation module currently under development, which makes use of high intensity light emitting diodes. The unit is designed as an adaption for a conventional high temperature oven used in TL dating; the characteristics of the device, and its potential for application to PL dating is assessed.

Introduction

The use of low energy photons in stimulating higher energy luminescence for probing the mechanisms of luminescence and the nature of defects is well established (see Curie, 1963). Huntley et al (1985) showed that such anti-Stokes emission, excited by 514 nm laser radiation, could potentially be used as a tool for dating, an observation which was quickly taken up by others (Smith et al, 1986; Rhodes, 1988). Godfrey-Smith et al (1988) found that IR radiation could excite luminescence in both feldspar and quartz, also demonstrating that this could be excited in feldspar using an LED (880 nm; FWHM 100nm). Although excitation with such low energy photons was unexpected, Hütt et al (1988), who had also studied this effect, found that the mechanism of electron eviction was phonon-assisted. In a detailed study of K-feldspar, they measured the low energy photo-stimulation spectrum ($2.4 < h\upsilon < 1.1$ eV) whilst monitoring the high energy luminescence emitted from the sample. The stimulation spectrum displayed several resonant excitations peaking at 1.29, 1.33, 1.43 and 2.25 eV, leading to direct optical ionization of the centre at 2.5 eV. The lower energy resonances were interpreted as transitions from the ground state to a sequence of excited states, where electrons could be elevated to the conduction band by phonon absorption. The thermal trap depth of these defects was also determined, and found to be of the order of 2 eV, suggesting suitability for dating. This was substantiated in their paper by preliminary age determination results for a number of sediment samples. We have developed the above observations by assessing the suitability of LEDs emitting at 950 nm (FWHM 100nm) for use in practical dating applications.

Experimental Details

A variety of LED's are commercially available, broadly being grouped into the very high intensity infra-red sources (based on GaAs), or near IR/red (AlGaAs), to the lower intensity visible devices (green/red) based on GaP. They are made by most of the major electronic device manufacturers and, in the UK, prices range from £0.3 to £2.5 each. We have so far used both green and infra-red diodes, having considerably more success with the latter. Results are described for the use of 15 mW, 950 nm (1.3 eV) GaAs LEDs (Telefunken TSUS 5402).

Sixteen diodes were arranged in a circular array around the sample, mounted at 30° to the horizontal. Luminescence emitted perpendicularly through this ring was monitored with the same PM tube as used in the TL measurements, with the addition of Schott BG38 filters to reject the scattered IR radiation. This simple set-up is shown in figure 1. The dimensions were chosen for low light loss when exciting samples deposited on 10mm diameter discs. Beam uniformity across a section of such a disc is shown in fig 2, as determined by optical bleaching of charge trapped in a 1x1x0.1mm crystal of geological K-feldspar.

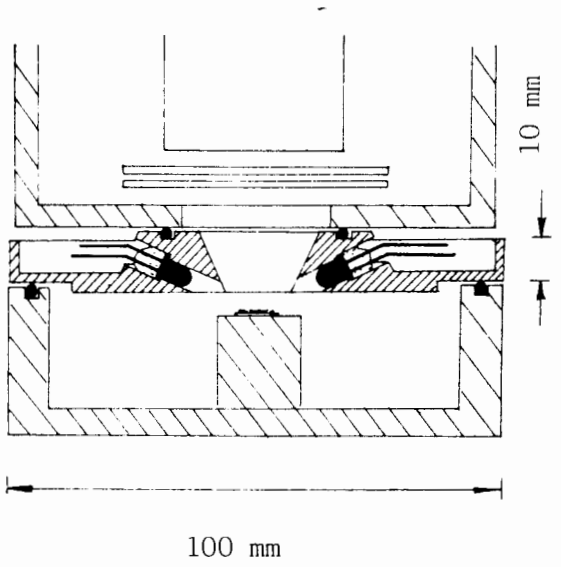

Figure1
Cross-section of the diode array described in the text. The device is used as an adaptation to an existing TL oven (lower part of the figure), inserted below the photomultiplier tube (top). The 16 LEDs are fixed with silicone sealant to cut out stray light, and allow the oven chamber to be evacuated, if necessary. Typical dimensions of the module are shown.

The LEDs were connected in parallel to a current limiting DC power supply. The initial light output of the LEDs (as measured by radiation scattered from a "white" paper disc) was in proportion to the current, up to the maximum ratings of the devices. If the current was limited to less than 1 A (the recommended typical operating value), then the light output was proportional to the power supplied (figures 3a&b). However, for higher values of current, a transient was observed upon switching on (figure 3c&d), settling down to an equilibrium output after approximately 10 s. For lower

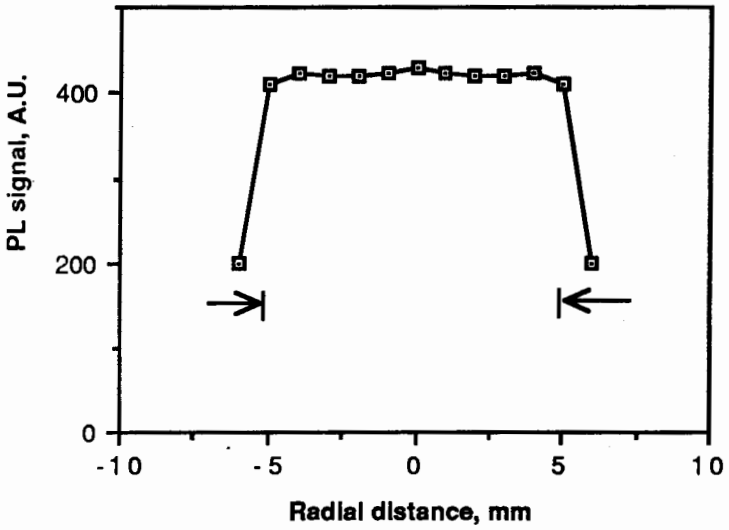

Figure 2
Radial uniformity of the excitation source of the 16 LEDs aranged in a circular array, as shown in figure 1. The markers indicate the dimensions of the sample discs used.

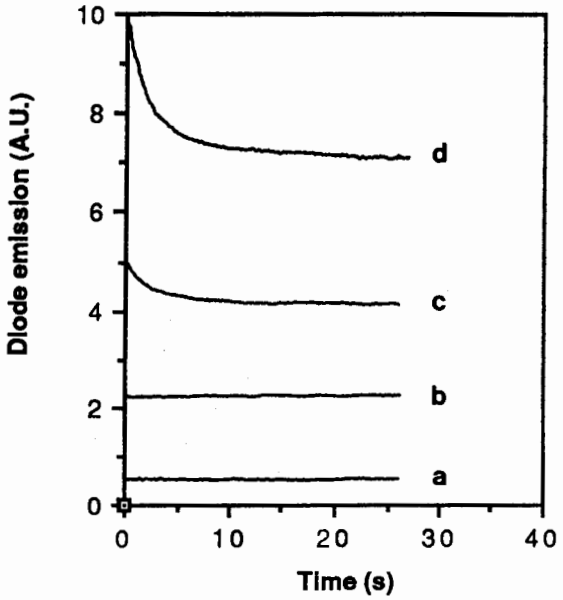

Figure 3
Light output characteristics of the LEDs with increasing current throughput; a)0.25A(1.2V); b) 0.85A (1.4V); c) 1.55A(1.6V); d) 3.0A (2.0V). Values are for the array of 16 diodes.

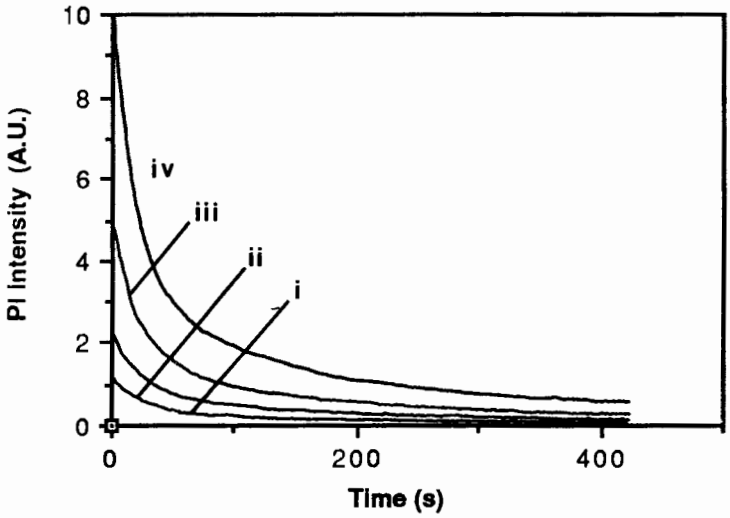

Figure 4

a) Time decay characteristics of IR stimulated luminescence of K-feldspar having received various beta doses (see text). The initial count-rate of curve iv was 50 kcps.

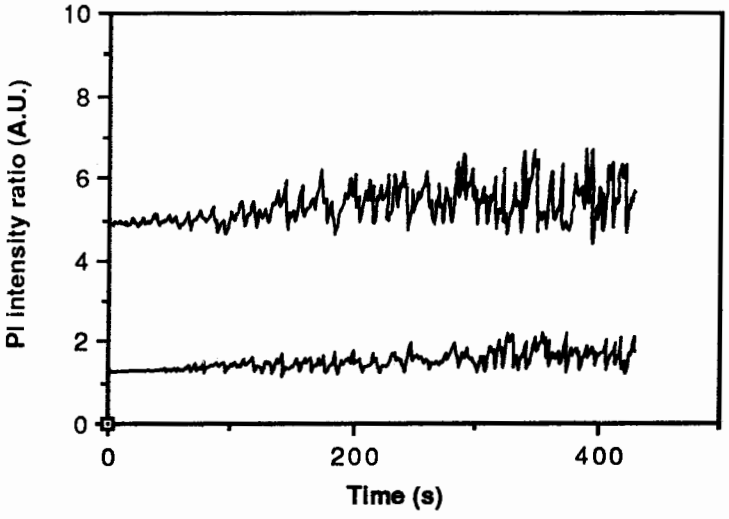

b) Ratio of the PL curves ii and iv shown in a), with respect to curve i.

values of current, this equilibrium was as stable as the power supply (in our case, constant to within experimental measurement determination of ±0.5%). For practical dating applications, the current was limited to be at or below 1 A, yielding estimated excitation powers at the sample of less than 60 mW cm^{-2}. It is also noted that these devices have good switch on/off characteristics which make them suitable for pulsed operation.

Discussion

Using infra-red radiation to induce ionization of traps stable over archaeological times, requires a more complex mechanism than direct photo-eviction, and one possibility is discussed by Hutt et al (*ibid*). These processes may therefore only be found in a limited number of materials. The samples we have so far studied which showed IR stimulated emission (where the laboratory doses administered were typical for archaeological material) were Na and K-feldspars, and pink quartz. By far the strongest luminescence, however, is stimulated in the K-feldspars, and it is in the dating of these minerals that we envisage the device to be most practicable.

The preliminary results of dose-response tests performed using 90-150 μm sedimentary K-feldspar are shown in figure 4. Using a simulation dose of 1.6 Gy and a regeneration procedure, values of ED of a) 1.58 ± 0.01 Gy and b) 1.55 ± 0.03 Gy were obtained. The basis for these calculations were a) using the ratios of the PL intensities measured at 1 s intervals between 0 and 10s after switch on, and b) using the ratios of the integrated PL intensities to a time where the intensity was less than 2% of the initial value. The difference in the results obtained using these two methods of analysis is, in this case, not significant. However, analysis of the decay curves for the above and other sedimentary feldspar samples has revealed that the form of the decay may be dose dependent. This is most easily seen when comparing the values of integrated PL (normalised to equal dose) plotted against time. Where such differences are significant, values of ED obtained as a function of exposure time (see Rhodes, 1988) using PL intensity ratios will show a systematic variation.

The real potential of the PL module in dating young sediments is still under assessment, but initial results look encouraging. One sample examined was a fine-grain marine sediment, extracted from Samsø, Denmark, (carbon dated to 3760+/-95 bc (K-4002)). XRD analysis indicated the presence of quartz and equal quantities of plagioclase and K- feldspars. By using bleach-regeneration (using bleach wavelengths longer than 500 nm) and additive dose techniques for measurement of palaeodose, apparent ages of 3870 ±750 and 4920 ± 690 BC respectively were produced when using the integrated curve as a measure of trapped charge (fading tests are in progress). Although these initial results are encouraging, further investigations are clearly needed.

Conclusion

The characteristics of 950 nm emitting diodes for use as PL excitation sources makes them potentially suitable in dating applications. A particular advantage of using IR compared with visible excitation is the reduced problem of rejecting excitation wavelengths, where a blue/uv biassed photomultipliers are employed for detection. The potential also exists for using a set of LEDs emitting at different wavelengths (or dual colour LEDs) mounted in the same array for selectively exciting individual mineral components within a polymineral sample. However, if this is to be successful, much more needs to be known about the charge trapping and transfer mechanisms in the relevant minerals.

Acknowledgements

The modules were constructed in the University Mechanical Workshop, and this work forms part of a research project suported by the Science-based Archaeology Committee of the SERC, and the University of Durham.

References

Curie D. (1963)*Luminescence in Crystals.* Methuen and Co, London.

Godfrey-Smith D.I., Huntley D.J., Chen W.H. (1988) Optical dating studies of quartz and feldspar sediment extracts. *Quaternary Sci Rev.*, 7, 373-380.

Huntley D.J., Godfrey-Smith D.I., Thewalt M.L.W. (1985) Optical dating of sediments. *Nature*, 313 105-108.

Hütt, G., Jaek I., Tchonka, J. (1988) Optical dating: K-feldspars optical response stimulation spectra. *Quatern. Sci Rev.*, 7, 381-385.

Rhodes E.J. (1988) Methodological considerations in the optical dating of quartz. *Quatern. Sci Rev.*, 7, 395 - 400.

Smith B.W., Aitken M.J., Rhodes E.J., Robinson P.D. (1986) Optical dating: methodological aspects. *Radiation Protection Dosimetry*, 17, 229-233.

PI Reviewer's Comments (Ann Wintle)

The use of cheap LEDs for stimulating luminescence in minerals extracted from sediments opens up a new field of study, which, when carried out in parallel with TL studies, will lead to a greater understanding of the basic mechanisms. This study developed from the very interesting paper given by Galina Hütt at the Cambridge meeting in 1987.

Computer Column/Bibliography/ Editorial

A review of Data Acquisition boards for the Apple Macintosh by Ed Haskell

If your have a Macintosh (Mac) in your laboratory you probably use it for word processing, spreadsheet analysis, and graphics, but not for data acquisition. The Mac got off to a slow start in that area. It was released without a compiler, was difficult to program when compilers were made available, and, until the SE was released it didn't have any expansion slots to which high-speed data acquisition peripherals could be attached. Well, things have changed and now you can hook up your Mac to the equipment you use for data-acquisition or you can replace that equipment entirely with off the shelf or custom designed data acquisition and controller boards from a variety of Macintosh vendors. You can also choose the degree of programming you feel capable of, from high-level Icon-based programming using National Instruments' LabVIEW, to low-level programming at the board and chip level using the NuBus prototyping board from Diversified I/O. And you can acquire your data using anything from the Mac 512 to the Mac II.

National Instruments NB series of Nubus boards for the Mac II

National Instruments is well established in the data-acquisition and control systems, providing boards for most bus architectures including Digital Equipment's UNIBUS and Q-Bus, the VMEbus, MULTIBUS, STD Bus, S-100, IBM PC and PS/2, and Apollo 3000/AT. It also produces products for the serial port on the Mac 512 as well as cards for the Mac SE and the Mac II. National Instruments provides perhaps the most powerful and comprehensive set of D/A, A/D, digital I/O, GPIB and multifunction boards available for the Mac II. Enhanced by DMA (Direct Memory Access) and their Real-Time System Integration feature (RTSI, which provides high speed inter-board timing controls). These boards provide "complex system board measurements never before possible on a personal computer", according to the manufacturer. National Instruments Mac II boards include:

NB-GPIB The NB-GPIB is an IEEE-488 interface board which enables data transfers between the Mac II and any of the thousands of IEEE-488 compatible instruments. A Mac II equipped with the NB-GPIB can be connected to up to 13 engineering, scientific, or medical instruments and can function under the LabVIEW software construction system (more on LabVIEW later) as well as conventional languages such as C, BASIC, FORTRAN, Pascal and Assembly. The NB-GPIB can reach transfer speeds of up to 1M bytes/sec when used with the RTSI and DMA capability of the (optional) NB-DMA-8-G board.

NB-MIO-16 The NB-MIO-16 is a multifunction analog, digital, and timing input/output board. It contains a 12-bit (4K intervals) A/D converter with up to 16 analog inputs and sample rates of up to 111K samples/sec, two 12-bit D/A converters; 8 lines of TTL-compatible digital I/O, and three 16-bit counter/timer channels for frequency counting, event counting, and pulse output applications.

NB-AO-6 The NB-AO-6 consists of six identical D/A converter channels each of which has a 4-20mA current output and a voltage output. The NB-AO-6 when used with the NB-DMA-8-G board can simultaneously generate six different waveforms at sample rates up to 300 kHz. These waveforms can be synchronized with functions of the other NB series boards using the capabilities of the RTSI bus interface.

NB-DIO-32F The NB-DIO-32F is a high-speed 32-bit parallel digital I/O board. The 32 lines of digital I/O are divided into four bytes and each byte can be programmed as either an input or an output port. This board, with its variety of digital I/O handshaking options enables the Mac II to function as a system controller with high-speed digital I/O capabilities for a wide variety of laboratory applications.

NB-DIO-24 The NB-DIO-24 is a lower priced 24-bit parallel digital I/O board which can operate in either unidirectional or bidirectional mode and can generate interrupt request outputs to peripheral devices. It is the only board of the NB series which cannot use the RTSI bus trigger lines for inter-board synchronization.

NB-DMA-8-G The NB-DMA-8-G is a multifunction interface board which provides DMA data transfer support for the other NB series boards by means of the RTSI bus. It also provides RTSI bus timing and interrupt support to integrate and synchronize the operations of other NB boards. The NB-DMA-8-G has a built-in IEEE-488 interface capable of transfer rates of up to 1 Mbytes/sec (compatible with the fastest IEEE-488 instruments).

Programming the NB series boards

LabDriver Software from National Instruments provides the driver routines for the NB board functions that can be called from the user's application programs. LabDriver is installed with a utility into the user's operating system and can then be accessed directly from any language that supports system toolbox device manager calls (most of them). Language interface libraries which provide even easier access to the routines are presently available for Lightspeed C, MPW C and MS BASIC. An important feature of the LabDriver Software is the ease with which DMA transfers are handled when the NB-DMA-8-G board is installed. The same routines which use interrupt-driven transfers when the NB-DMA-8-G is not installed automatically implement DMA transfers when it is connected, invisible to the software user. Aside from routines for directly controlling the A/D, D/A, digital I/O and timing functions of the NB boards, the LabDriver

Software provides high-level routines which allow the user to perform high-speed timing I/O functions such as pulse generation, frequency generation, event counting and timed process control when used with the NB-DMA-8-G board. Routines are also available for use with the RTSI bus trigger lines allowing boards to share clocks and signals between boards and to synchronize board operations.

Boards for the Mac SE

GPIB-SE The GPIB-SE is an IEEE-488 interface board for the Mac SE with optional MC-68881 floating point coprocessor and DMA controller. The GPIB-SE hardware consists of a plug-in circuit card and a 7 inch ribbon cable that connects the board to an IEEE-488 connector that mounts on the back of the Mac SE case. Transfer rates of between 2k to 200 kbytes/sec are achieved with the basic unit (without DMA) depending on software driver and instrumentation. With DMA, maximum *reads* from a GPIB device are 1 Mbytes/sec and *writes* to a GPIB device at 700 kbytes/sec. The GPIB-SE comes with the National Instruments NI-488 software package which contains a set of BPIB routines accessed from most programming languages through system calls. High-level interfaces are available for MPW C, MS BASIC and MS FORTRAN. LabVIEW software can also be used with the GPIB-SE.

Serial Interfaces

GPIB-422CV The GPIB-422CV (the 'Micro Box') is basically an IEEE-488 converter box which allows any Macintosh computer (including the 128k Mac) to control a single GPIB device. The GPIB-422CV communicates with the Mac at a maximum rate of 5 kbaud, but can transfer buffered data to the GPIB device at up to 900 kbytes/sec. The box can be powered from an external supply or by batteries. The standard unit comes with 64 kbytes of RAM buffer and can be expanded to 256 kbytes. This unit can act as a dedicated GPIB controller when left connected to the Mac, or it can be disconnected from the Mac after data downloading and act as a high speed buffer for driving CAD/CAM devices such as large plotters. The GPIB-422CV can be used with LabVIEW software, however no more than one device may be connected at a time.

GPIB-MAC The GPIB-Mac was the first IEEE-488 controller available for the Mac. This unit can also be used with the 128k Mac although to use it with the LabView software requires at least 1 Mbyte of memory. The GPIB-MAC comes with buffer sizes of from 2 kbytes to 32 kbytes. Data transfer rates are limited by the rate of data exchange on the Mac RS-422 serial port. The GPIB-MAC can control up to 13 IEEE-488 devices.

LabVIEW Software

LabVIEW is a unique programming environment developed by National Instruments (and now licensed to other board makers) which frees the programmer from the low level routines required for programming in C, Pascal, FORTRAN, Basic etc. LabView provides pre-designed graphics output modules for the data being collected as well as 'virtual' control panels for controlling equipment directly from the Macintosh screen. The functions needed from a number of GPIB instruments can be consolidated into a single 'virtual instrument' on the Mac screen, and a single Icon representing this new arrangement can be stored and used in conjunction with other functions or instruments in future applications. Programming with LabView is 'data flow oriented' and is accomplished by connecting the inputs and outputs of pre-designed and custom built icons corresponding to the functions of the instruments being controlled. Complex statistical, matrix, signal processing and database functions are also Icon based and can be used for analysis of data collected through the GPIB bus or input from other programs such as Microsoft Excel. Before external equipment is connected to the Mac a virtual instrument can be constructed and computer generated data can be used to test the program. This feature makes LabVIEW well suited for prototyping and educational uses. LabVIEW can also be used with the NB series of boards which provide non-GPIB functions.

For further details contact: National Instruments Corp. 12109 Technology Blvd. Austin, Texas 78727-6204 USA (512) 250-9119 (800) 531-4742

Bibliography

Mejdahl, V. (1988) A survey of archaeological samples dated in 1987. Risø National Laboratory Publication M-2175. ISBN 87-550-1426-7. 34pp.

Grün, R. (1989) Die ESR-Altersbestimmungsmethode. Springer Verlag, Berlin. ISBN 3-540-50146-0. (In German).

Editorial

* Readers will have noticed an unfortunate typographical error in the item on electronic mail and Fax communications in the last issue of Ancient TL. The country prefix to Dave Huntley's Fax # was given as USA and not Canada, as it should have been. This was a genuine error, and I offer my unreserved apologies, and trust that diplomatic relations can now be restored.

* Some articles are travelling a circuitous route before they reach me for first submission. I should be grateful if authors would take note of the guidelines, particularly the requirements concerning the Reviewer's report which must accompany the final version of an accepted paper.

* New Date List entry forms are now available from Durham which enable simplified entry of data for multiple date entries. For those who use Macintosh computers, the data entries can also be made using Excel and Word skeleton worksheets /documents. The first compilation for archaeologists is due this year.

* The Editor wishes to thank Paul Larsen, Romola Parish and Nigel Poolton for their help in the production of this issue of *Ancient TL*.